J|A|C|S
ARTICLES
Published on Web 11/16/2002

Organic Triplet Emissions of Arylacetylide Moieties Harnessed through Coordination to $[Au(PCy_3)]^+$. Effect of Molecular Structure upon Photoluminescent Properties

Hsiu-Yi Chao, Wei Lu, Yanqin Li, Michael C. W. Chan, Chi-Ming Che,* Kung-Kai Cheung, and Nianyong Zhu

Contribution from Department of Chemistry and HKU−CAS Joint Laboratory on New Materials, The University of Hong Kong, Pokfulam Road, Hong Kong SAR, China

Received July 9, 2002

Abstract: A family of mono- and binuclear Cy_3P-supported gold(I) complexes containing various π-conjugated linear arylacetylide ligands, including the two homologous series $(Cy_3P)Au(C{\equiv}CC_6H_4)_{n-1}(C{\equiv}CPh)$ and $(Cy_3P)Au(C{\equiv}CC_6H_4)_nC{\equiv}CAu(PCy_3)$ ($n = 1-4$), have been prepared. X-ray crystal analyses revealed no intermolecular aurophilic interactions in their crystal lattice. The lowest-energy singlet transitions are predominately intraligand in nature and exhibit both phenyl and acetylenic $^1(\pi\pi^*)$ character. Strong photoluminescence is detected in solid and solution states under ambient conditions, with lifetimes in the microsecond regime. For complexes with a single arylacetylide group, only phosphorescence from the arylacetylide $^3(\pi\pi^*)$ state is observed. Vibrational spacings in the solid-state emission spectra can be attributed to a combination of phenyl ring deformation and symmetric phenyl ring and C≡C stretches. Additional delayed-fluorescence emission is recorded for complexes with multiple *p*-arylacetylide units, and this is attributed to a triplet−triplet annihilation process. The phosphorescence energy of these complexes are readily modified by altering the length of the conjugated arylacetylide system, while the intensity of phosphorescence relative to fluorescence decreases when the *p*-arylacetylide chain is elongated. Information regarding the nature and relative energies of arylacetylide singlet and triplet excited states has been derived from the two homologous series and extrapolated to polymeric arylacetylide species. The $^3(\pi\pi^*)$ excited-state reduction potentials E° [$\mathbf{Au}^+/\mathbf{Au}^*$] (**Au** = **1a**, **2**, and **4**) are estimated to be −1.80, −1.28, and −1.17 V versus SSCE, respectively.

Introduction

The search for new classes of organic and metal-organic compounds with optoelectronic applications in materials science has intensified in the past few years. Conjugated ethynylated materials, such as arylacetylenes,[1] poly(arylene-ethynylene)s,[2] and metal-containing acetylide complexes[3] and polymers,[4] have been investigated for their nonlinear optical (NLO), liquid crystalline, electroluminescent, conducting, and electron/energy transfer properties. From a photophysical viewpoint, arylacetylenes do not display long-lived triplet emissions under ambient conditions and phenylacetylene is virtually nonemissive at wavelengths above 400 nm. Recent studies on fluorescence-based poly(*p*-phenylene-ethynylene)s (PPEs) have elegantly demonstrated that controlled manipulation of the polymer conformation can yield intriguing photophysical changes,[2] while

* To whom correspondence should be addressed. E-mail: cmche@hku.hk.

(1) (a) Martin, R. E.; Diederich, F. *Angew. Chem., Int. Ed.* **1999**, *38*, 1350−1377. (b) Stang, P. J.; Diederich, F. *Modern Acetylene Chemistry*; VCH: Weinheim, Germany, 1995. (c) Carter, G. M.; Chen, Y. J.; Rubner, M. F.; Sandman, D. J.; Thakur, M. K.; Tripathy, S. K. In *Non-Linear Optical Properties of Organic Molecules and Crystals*; Chemla, D. S., Zyss, J., Eds.; Academic: Orlando, FL, 1987; Vol. 2, Chapter III-3, p 85.

(2) (a) Beeby, A.; Findlay, K.; Low, P. J.; Marder, T. B. *J. Am. Chem. Soc.* **2002**, *124*, 8280−8284. (b) Kim, J.; Levitsky, I. A.; McQuade, D. T.; Swager, T. M. *J. Am. Chem. Soc.* **2002**, *124*, 7710−7718. (c) Cornil, J.; Karzazi, Y.; Brédas, J. L. *J. Am. Chem. Soc.* **2002**, *124*, 3516−3517. (d) Sluch, M. I.; Godt, A.; Bunz, U. H. F.; Berg, M. A. *J. Am. Chem. Soc.* **2001**, *123*, 6447−6448. (e) Levitus, M.; Schmieder, K.; Ricks, H.; Shimizu, K. D.; Bunz, U. H. F.; Garcia-Garibay, M. A. *J. Am. Chem. Soc.* **2001**, *123*, 4259−4265. (f) Tour, J. M. *Acc. Chem. Res.* **2000**, *33*, 791−804. (g) Bunz, U. H. F. *Chem. Rev.* **2000**, *100*, 1605−1644. (h) McQuade, D. T.; Kim, J.; Swager, T. M. *J. Am. Chem. Soc.* **2000**, *122*, 5885−5886. (i) Deans, R.; Kim, J.; Machacek, M. R.; Swager, T. M. *J. Am. Chem. Soc.* **2000**, *122*, 8565−8566. (j) Sato, T.; Jiang, D. L.; Aida, T. *J. Am. Chem. Soc.* **1999**, *121*, 10658−10659. (k) Yang, J. S.; Swager, T. M. *J. Am. Chem. Soc.* **1998**, *120*, 11864−11873. (l) Montali, A.; Bastiaansen, C.; Smith, P.; Weder, C. *Nature* **1998**, *392*, 261−264. (m) Pang, Y.; Li, J.; Hu, B.; Karasz, F. E. *Macromolecules*, **1998**, *31*, 6730−6732. (n) Moore, J. S. *Acc. Chem. Res.* **1997**, *30*, 402−413.

(3) (a) Manna, J.; John, K. D.; Hopkins, M. D. *Adv. Organomet. Chem.* **1995**, *38*, 79−154. (b) Fujikura, Y.; Sonogashira, K.; Hagihara, N. *Chem. Lett.* **1975**, 1067−1070. (c) Ma, Y. G.; Chan, W. H.; Zhou, X. M.; Che, C. M. *New J. Chem.* **1999**, *23*, 263−265. (d) Chan, S. C.; Chan, M. C. W.; Wang, Y.; Che, C. M.; Cheung, K. K.; Zhu, N. *Chem.—Eur. J.* **2001**, *7*, 4180−4190. (e) Lu, W.; Mi, B. X.; Chan, M. C. W.; Hui, Z.; Zhu, N.; Lee, S. T.; Che, C. M. *Chem. Commun*. **2002**, 206−207. (f) Long, N. J. In *Optoelectronic Properties of Inorganic Compounds*; Roundhill, D. M., Fackler, J. P., Jr., Eds.; Plenum Press: New York, 1999; Chapter 4. (g) Mingos, D. M. P.; Yau, J.; Menzer, S.; Williams., D. J. *Angew. Chem., Int. Ed. Engl.* **1995**, *34*, 1894−1895. (h) Lavastre, O.; Plass, J.; Bachmann, P.; Guesmi, S.; Moinet, C.; Dixneuf, P. H. *Organometallics* **1997**, *16*, 184−189. (i) McDonagh, A. M.; Humphrey, M. G.; Samoc, M.; Luther-Davies, B.; Houbrechts, S.; Wada, T.; Sasabe, H.; Persoons, A. *J. Am. Chem. Soc.* **1999**, *121*, 1405−1406. (j) John, K. D.; Hopkins, M. D. *Chem. Commun*. **1999**, 589−590. (k) Walters, K. A.; Dattelbaum, D. M.; Ley, K. D.; Schoonover, J. R.; Meyer, T. J.; Schanze, K. S. *Chem. Commun*. **2001**, 1834−1835.

10.1021/ja0209417 CCC: $22.00

applications in molecular electronics and sensory technology have also been developed. Nevertheless, the triplet excited states of arylacetylide groups and PPEs have not been fully elucidated. A thorough understanding of their excited-state properties is required before a rational design approach for π-conjugated polymers can be realized. In this context, Hopkins has presented a review on the bonding of metal−alkynyl complexes and discussed the impact of the metal upon electronic transitions involving the arylacetylide orbitals.[3a]

We envisaged that if the emission from the triplet excited states of arylacetylides can be "switched on" under ambient conditions, such compounds and their polymeric forms may be exploited as emitting materials in organic light-emitting devices (OLEDs) and luminescent sensors. One possible strategy to achieve this is by ligation to heavy metal ions, which introduces spin−orbit coupling. Friend and co-workers have previously incorporated the $Pt(PR_3)_2$ moiety (R = alkyl) into π-conjugated polymers to give rigid-rod organometallic chains such as $[-Pt(P^nBu_3)_2-C\equiv C-R'-C\equiv C-]_\infty$ (R′ = alkyl or heteroaromatic ring(s)), and triplet $\pi\pi^*$ emissions have been observed at low temperatures.[4a−f] However, the low-energy d−d excited state for Pt(II), which provides a facile means for nonradiative decay, is a major obstacle for observing the triplet emission of these polymers in solution. In this regard, Au(I) is a sagacious choice because the d^{10} closed-shell configuration does not allow low-lying d−d excited states. The photoluminescence of gold(I) arylacetylide derivatives has been studied by several groups.[5] Nevertheless, observations of $^3(\pi\pi^*)$ emissions in these systems are habitually complicated by intraligand excited states of auxiliary phosphine ligands and by metal-centered excited states arising from metal−ligand and/or metal−metal bonded exciplex formation. The intraligand $^3(\pi\pi^*)$ state is of particular interest because its energy can be readily tuned through electronic modification of the arylacetylide moiety.

Our recent reports on the binuclear Au(I) complexes $Cy_3PAu(C\equiv C)_nAuPCy_3$ (PCy_3 = tricyclohexylphosphine; $n = 1-4$) have established the nature of $^3(\pi\pi^*)$ emissions originating from the bridging $(C_{2n})^{2-}$ units.[6] Tricyclohexylphosphine is a judicious ancillary group for these studies because it has no low-lying ligand-localized excited states and its bulkiness disfavors metal−metal and $\pi-\pi$ oligomerization processes. We now present the synthesis and structural and spectroscopic properties of a family of mono- and binuclear PCy_3-supported gold(I) arylacetylide complexes that are strongly luminescent. The characteristics of the triplet excited states of organic arylacetylides will be described in detail. By probing the $^3(\pi\pi^*)$ emissions of the two homologous series $Cy_3PAu(-C\equiv C-Ar)_n$ and $Cy_3PAu(C\equiv C-Ar)_nC\equiv CAuPCy_3$ ($n = 1-4$), it is anticipated that a structure−function (i.e. photoluminescence) relationship can be established and valuable insight into the photophysical nature of $(-C\equiv C-Ar-)_n$ materials can be derived.

Experimental Section

Materials. All starting materials were purchased from commercial sources and used as received unless stated otherwise. The solvents used for synthesis were of analytical grade. Details of solvent treatment for photophysical studies have been described earlier.[7] Trimethylamine and diethylamine were freshly distilled over KOH pellets. HC≡CC≡CPh,[8] 1,4-diethynylbenzene,[9] HC≡C-1,4-C_6H_4-1,4-C_6H_4C≡CH,[9] 4-ethynylpyridine,[10] HC≡C-1,4-C_6H_4Ph,[11] $Me_3Si(C\equiv C\text{-}1,4\text{-}C_6H_4)_3C\equiv CSiMe_3$,[11] $Me_3SiC\equiv C\text{-}1,4\text{-}C_6H_4-C\equiv CSi^iPr_3$,[12] and $Au(PCy_3)Cl$[13] were prepared according to literature procedures. The synthesis of $Me_3SiC\equiv C\text{-}1,4\text{-}C_6H_4C\equiv CPh$ was the same as that of (4-ethynylphenyl)(4′-pyridyl)-acetylene except phenylacetylene was used instead of 4-ethynylpyridine.[14] $H(C\equiv C\text{-}1,4\text{-}C_6H_4)_2C\equiv CH$ was prepared by desilylation from $Me_3Si(C\equiv C\text{-}1,4\text{-}C_6H_4)_2C\equiv CSi^iPr_3$ with tetrabutylammonium fluoride in aqueous THF.[12] $Me_3Si(C\equiv C\text{-}1,4\text{-}C_6H_4)_2C\equiv CPh$, $Me_3Si(C\equiv C\text{-}1,4\text{-}C_6H_4)_3C\equiv CPh$, and $Me_3Si(C\equiv C\text{-}1,4\text{-}C_6H_4)_4C\equiv CSiMe_3$ were synthesized from the reaction of [(4-iodophenyl)ethynyl]trimethylsilane with 1-ethynyl-4-(phenylethynyl)benzene, $H(C\equiv C\text{-}1,4\text{-}C_6H_4)_2C\equiv CPh$, and $H(C\equiv C\text{-}1,4\text{-}C_6H_4)_2C\equiv CH$, respectively.[14]

Synthesis. Full experimental and characterization data for complexes **1**−**12** are given in the Supporting Information. Synthetic details for **1a**, **6**, and **8** are provided here as examples. The procedure for **1a** was adopted for the synthesis of **1b**−**1d**, **2**−**5**, and **7** using the corresponding acetylenes or trimethylsilylacetylenes in the presence of NaOMe or KOH. The procedure for **6** was adopted for the synthesis of **12** using $Me_3Si(C\equiv C\text{-}1,4\text{-}C_6H_4)_4C\equiv CSiMe_3$ in the presence of KOH. The procedure for **8** was adopted for the synthesis of **9**−**11** using the corresponding diacetylenes or trimethylsilyldiacetylenes in the presence of NaOMe or KOH.

Au(PCy_3)(C≡CPh) (1a). A solution of $Au(PCy_3)Cl$ (0.10 g, 0.20 mmol) in CH_2Cl_2/MeOH (1:1, 30 mL) was treated with phenylacetylene (0.02 g, 0.20 mmol) and excess NaOMe (0.02 g, 0.37 mmol) in MeOH (5 mL). The mixture was stirred at room temperature for 3 h. After evaporation to dryness, the solid residue was extracted with CH_2Cl_2. Diffusion of diethyl ether into the concentrated solution gave colorless crystals. Yield 0.07 g (62%). ^1H NMR ($CDCl_3$) δ 7.51−7.48 (m, 2H, phenyl), 7.25−7.15 (m, 3H, phenyl), 2.08−1.18 (m, 33H, Cy); $^{13}C\{^1H\}$ NMR ($CDCl_3$) δ 136.1 (d, $^2J_{CP}$ = 131 Hz, Au−**C**≡C), 132.1, 127.6, 126.3, 125.0, 103.4 (d, $^3J_{CP}$ = 25 Hz, Au−C≡**C**), 33.2 (d, $^1J_{CP}$ = 27 Hz, Cy), 30.7 (s, Cy), 27.1 (d, $^2J_{CP}$ = 12 Hz, Cy), 25.9 (s, Cy);

(4) (a) Wittmann, H. F.; Friend, R. H.; Khan, M. S.; Lewis, J. *J. Chem. Phys.* **1994**, *101*, 2693−2698. (b) Younus, M.; Köhler, A.; Cron, S.; Chawdhury, N.; Al-Mandhary, M. R. A.; Khan, M. S.; Lewis, J.; Long, N. J.; Friend, R. H.; Raithby, P. R. *Angew. Chem., Int. Ed.* **1998**, *37*, 3036−3039. (c) Chawdhury, N.; Köhler, A.; Friend, R. H.; Wong, W. Y.; Lewis, J.; Younus, M.; Raithby, P. R.; Corcoran, T. C.; Al-Mandhary, M. R. A.; Khan, M. S. *J. Chem. Phys.* **1999**, *110*, 4963−4970. (d) Wilson, J. S.; Köhler, A.; Friend, R. H.; Al-Suti, M. K.; Al-Mandhary, M. R. A.; Khan, M. S.; Raithby, P. R. *J. Chem. Phys.* **2000**, *113*, 7627−7634. (e) Wilson, J. S.; Chawdhury, N.; Al-Mandhary, M. R. A.; Younus, M.; Khan, M. S.; Raithby, P. R.; Köhler, A.; Friend, R. H. *J. Am. Chem. Soc.* **2001**, *123*, 9412−9417. (f) Köhler, A.; Wilson, J. S.; Friend, R. H.; Al-Suti, M. K.; Khan, M. S.; Gerhard, A.; Bässler, H. *J. Chem. Phys.* **2002**, *116*, 9457−9463. (g) Wilson, J. S.; Dhoot, A. S.; Seeley, A. J. A. B.; Khan, M. S.; Köhler, A.; Friend, R. H. *Nature* **2001**, *413*, 828−831. (h) Nguyen, P.; Gómez-Elipe, P.; Manners, I. *Chem. Rev.* **1999**, *99*, 1515−1548.

(5) For selected examples, see: (a) Li, D.; Hong, X.; Che, C. M.; Lo, W. C.; Peng, S. M. *J. Chem. Soc., Dalton Trans.* **1993**, 2929−2932. (b) Shieh, S. J.; Hong, X.; Peng, S. M.; Che, C. M. *J. Chem. Soc., Dalton Trans.* **1994**, 3067−3068. (c) Xiao, H.; Cheung, K. K.; Che, C. M. *J. Chem. Soc., Dalton Trans.* **1996**, 3699−3703. (d) Yam, V. W. W.; Choi, S. W. K. *J. Chem. Soc., Dalton Trans.* **1996**, 4227−4232. (e) Yam, V. W. W.; Choi, S. W. K.; Cheung, K. K. *Organometallics* **1996**, *15*, 1734−1739. (f) Tzeng, B. C.; Lo, W. C.; Che, C. M.; Peng, S. M. *Chem. Commun.* **1996**, 181−182. (g) Irwin, M. J.; Vittal, J. J.; Puddephatt, R. J. *Organometallics* **1997**, *16*, 3541−3547. (h) Hunks, W. J.; MacDonald, M. A.; Jennings, M. C.; Puddephatt, R. J. *Organometallics* **2000**, *19*, 5063−5070. (i) Lin, Y. Y.; Lai, S. W.; Che, C. M.; Cheung, K. K.; Zhou, Z. Y. *Organometallics* **2002**, *21*, 2275−2282.

(6) (a) Che, C. M.; Chao, H. Y.; Miskowski, V. M.; Li, Y.; Cheung, K. K. *J. Am. Chem. Soc.* **2001**, *123*, 4985−4991. (b) Lu, W.; Xiang, H. F.; Zhu, N.; Che, C. M. *Organometallics* **2002**, *21*, 2343−2346.

(7) Lai, S. W.; Chan, M. C. W.; Cheung, T. C.; Peng, S. M.; Che, C. M. *Inorg. Chem.* **1999**, *38*, 4046−4055.

(8) Kende, A. S.; Smith, C. A. *J. Org. Chem.* **1988**, *53*, 2655−2657.

(9) Takahashi, S.; Kuroyama, Y.; Sonogashira, K.; Hagihara, N. *Synthesis* **1980**, 627−630.

(10) Ciana, L. D.; Haim, A. *J. Heterocycl. Chem.* **1984**, *21*, 607−608.

(11) Khan, M. S.; Kakkar, A. K.; Long, N. J.; Lewis, J.; Raithby, P.; Nguyen, P.; Marder, T. B.; Wittmann, F.; Friend, R. H. *J. Mater. Chem.* **1994**, *4*, 1227−1232.

(12) Lavastre, O.; Ollivier, L.; Dixneuf, P. H.; Sibandhit, S. *Tetrahedron* **1996**, *52*, 5495−5504.

(13) Al-sa'ady, A. K.; McAuliffe, C. A.; Parish, R. V.; Sandbank, J. A. *Inorg. Synth.* **1985**, *23*, 191−194.

(14) Wu, I. Y.; Lin, J. T.; Luo, J.; Sun, S. S.; Li, C. S.; Lin, K. J.; Tsai, C.; Hsu, C. C.; Lin, J. L. *Organometallics* **1997**, *16*, 2038−2048.

Chart 1. Mononuclear and Binuclear Gold(I) Arylacetylide Complexes **1**−**12**

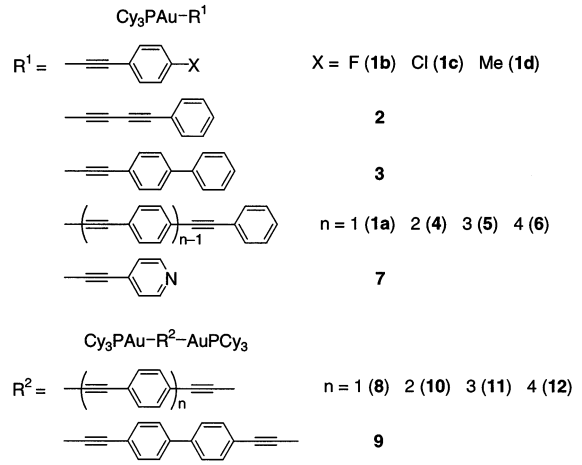

$^{31}P\{^1H\}$ NMR ($CDCl_3$) δ 57.49 (s). IR (KBr): 2113 cm^{-1} (w, C≡C). MS−FAB (+ve): *m*/*z* 579 [M^+]. Anal. Calcd for $C_{26}H_{38}AuP$: C, 53.96; H, 6.62. Found: C, 53.90; H, 6.59.

Au(PCy$_3$)[(C≡C-1,4-C$_6$H$_4$)$_3$C≡CPh] (6). A solution of Au(PCy_3)Cl (0.10 g, 0.20 mmol) in CH_2Cl_2/MeOH (1:1, 30 mL) was treated with $Me_3Si(C{\equiv}C\text{-}1,4\text{-}C_6H_4C)_3C{\equiv}CPh$ (0.1 g, 0.21 mmol) in THF (10 mL) and excess KOH (0.02 g, 0.36 mmol) in MeOH (10 mL). The reaction mixture was sonicated to assist the formation of a homogeneous solution. After filtration, the solution was evaporated to dryness. A light yellow product was obtained after purification by column chromatography (neutral alumina, CH_2Cl_2). Yield 0.14 g (82%). ^1H NMR (CD_2Cl_2) δ 7.57−7.37 (m, 17H, phenyl), 2.15−1.27 (m, 33H, Cy); $^{13}C\{^1H\}$ NMR (CD_2Cl_2) δ 142.3 (d, $^2J_{CP}$ = 132 Hz, Au−**C**≡C), 131.8, 131.5, 131.3, 128.6, 128.4, 126.3, 123.5, 123.3, 123.0, 122.9, 122.7, 120.5, 102.2 (d, $^3J_{CP}$ = 24 Hz, Au−C≡**C**), 91.6 (s, C≡C), 91.3 (s, C≡C), 90.9 (s, C≡C), 90.8 (s, C≡C), 89.9 (s, C≡C), 88.9 (s, C≡C), 33.2 (d, $^1J_{CP}$ = 28 Hz, Cy), 30.8 (s, Cy), 27.1 (d, $^2J_{CP}$ = 12 Hz, Cy), 26.0 (s, Cy); $^{31}P\{^1H\}$ NMR (CD_2Cl_2) δ 56.9 (s). IR (KBr): 2116 cm^{-1} (w, C≡C). MS−FAB (+ve): *m*/*z* 880 [M^+]. Anal. Calcd for $C_{50}H_{50}AuP{\cdot}(CH_2Cl_2)_{0.5}(H_2O)_{0.5}$: C, 65.20; H, 5.63. Found: C, 65.24; H, 5.50.

{**Au(PCy$_3$)**}$_2$(**μ-C≡C-1,4-C$_6$H$_4$C≡C) (8).** A solution of Au(PCy_3)Cl (0.15 g, 0.30 mmol) in CH_2Cl_2/MeOH (1:1, 40 mL) was treated with 1,4-diethynylbenzene (0.02 g, 0.16 mmol) and an excess of NaOMe (0.05 g, 0.93 mmol) in MeOH (10 mL). The mixture was stirred at room temperature for 3 h. After evaporating to dryness, the solid residue was extracted with CH_2Cl_2. Diffusion of diethyl ether into the concentrated solution gave colorless crystals. Yield 0.1 g (65%). ^1H NMR ($CDCl_3$) δ 7.34 (s, 4H, phenyl), 2.08−1.18 (m, 66H, Cy); $^{13}C\{^1H\}$ NMR ($CDCl_3$) δ 137.6 (d, $^2J_{CP}$ = 131 Hz, Au−**C**≡C), 131.6, 123.0, 103.6 (d, $^3J_{CP}$ = 24 Hz, Au−C≡**C**), 33.1 (d, $^1J_{CP}$ = 27 Hz, Cy), 30.6 (s, Cy), 27.1 (d, $^2J_{CP}$ = 8 Hz, Cy), 25.9 (s, Cy); $^{31}P\{^1H\}$ NMR ($CDCl_3$) δ 57.51 (s). IR (KBr): 2113 cm^{-1} (w, C≡C). MS−FAB (+ve): *m*/*z* 1079 [M^+]. Anal. Calcd for $C_{46}H_{70}Au_2P_2$: C, 51.19; H, 6.54. Found: C, 50.81; H, 6.30.

Results

Synthesis and Characterization. The mononuclear (**1**−**7**) and binuclear (**8**−**12**) gold(I) arylacetylide complexes were prepared by reacting Au(PCy_3)Cl with terminal acetylenes/trimethylsilylacetylenes (1:1) and diacetylenes/trimethylsilyldiacetylenes (2:1), respectively, in the presence of NaOMe or KOH.[15] Their structures are shown in Chart 1. These complexes are air-stable in the solid state and in solution. Aspects of their characterization data are highlighted here. Their IR spectra (KBr) show one to two weak ν(C≡C) bands at 2067−2207 cm^{-1}. The Raman spectra of the binuclear derivatives **8** and **9** exhibit an intense symmetric C≡C stretch at 2111 and 2107 cm^{-1}, respectively. The $^{13}C\{^1H\}$ NMR spectra of **1**(**a**−**d**) display two doublets at 137.9−135.3 ($^2J_{CP} \approx 131$ Hz) and 103.7−102.4 ($^3J_{CP} \approx 25$ Hz) ppm, which are assigned to the α- and *β*-acetylide carbon atoms, respectively. These α-acetylide chemical shifts are shifted downfield from that of Au(PCy_3)(C≡C^{t}Bu) (120.89 ppm),[16] and this can be attributed to the greater electron-donating ability of the *tert*-butyl group. The $^{31}P\{^1H\}$ NMR spectra of **1**−**12** reveal a singlet at 56.3−57.6 ppm, which is partially shifted downfield from that of Au(PCy_3)Cl (55.2 ppm).

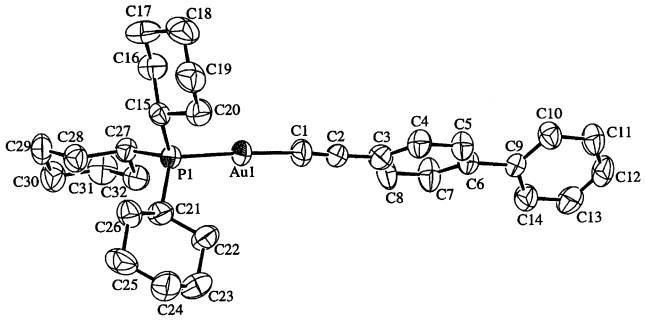

Figure 1. Perspective view of one of the two independent molecules of **3** (50% thermal ellipsoids). Selected bond lengths (Å) and angles (deg): Au(1)−P(1) 2.291(2), Au(1)−C(1) 2.003(7), C(1)≡C(2) 1.189(9), P(1)−Au(1)−C(1) 176.0(2), Au(1)−C(1)≡C(2) 175.7(8), C(1)≡C(2)−C(3) 177.7(9).

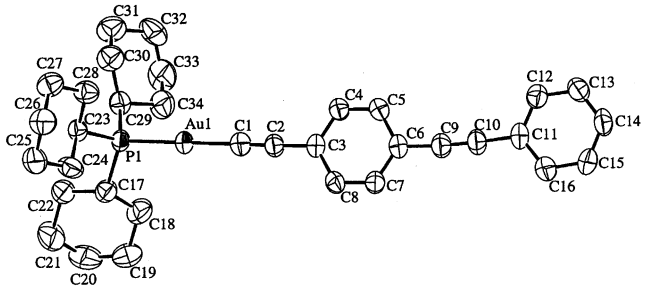

Figure 2. Perspective view of **4** (50% thermal ellipsoids). Selected bond lengths (Å) and angles (deg): Au(1)−P(1) 2.281(1), Au(1)−C(1) 2.007(5), C(1)≡C(2) 1.180(6), C(9)≡C(10) 1.188(6), P(1)−Au(1)−C(1) 178.2(1), Au(1)−C(1)≡C(2) 176.4(4), C(1)≡C(2)−C(3) 177.6(5), C(9)≡C(10)−C(11) 177.1(6).

The molecular structures of complexes **1a**−**d**, **2**−**5**, **7**, **8**, and **9**·MeOH·H_2O have been determined by X-ray crystal analyses. For **3**, **4**, and **9**·MeOH·H_2O, perspective drawings and selected bond lengths and angles are depicted in Figures 1−3, and crystal data are collected in Table 1 (see Supporting Information for details of other complexes). The Au(I) coordination geometry in all the structures are virtually linear with the P−Au−C angles ranging from 175.4(2)° to 178.7(4)°. The Au−P bond distances (2.281(1)−2.299(2) Å) are similar to those reported for gold(I) arylacetylide derivatives with triphenylphosphine ligands (2.263(3)−2.277(1) Å),[15a,c,17] and Au(PCy_3)Cl (2.242(4) Å).[18] The Au−C (1.993(11)−2.03(1) Å) and C(1)≡C(2) (1.180(6)−1.223(10) Å) distances of these complexes also resemble those

(15) (a) Bruce, M. I.; Horn, E.; Matisons, J. G.; Snow, M. R. *Aust. J. Chem.* **1984**, *37*, 1163−1170. (b) Cross, R. J.; Davidson, M. F. *J. Chem. Soc., Dalton Trans.* **1986**, 411−414. (c) Irwin, M. J.; Rendina, L. M.; Vittal, J. J.; Puddephatt, R. J. *Chem. Commun.* **1996**, 1281−1282.
(16) Vicente, J.; Chicote, M. T.; Abrisqueta, M. D.; Jones, P. G. *Organometallics* **1997**, *16*, 5628−5636.

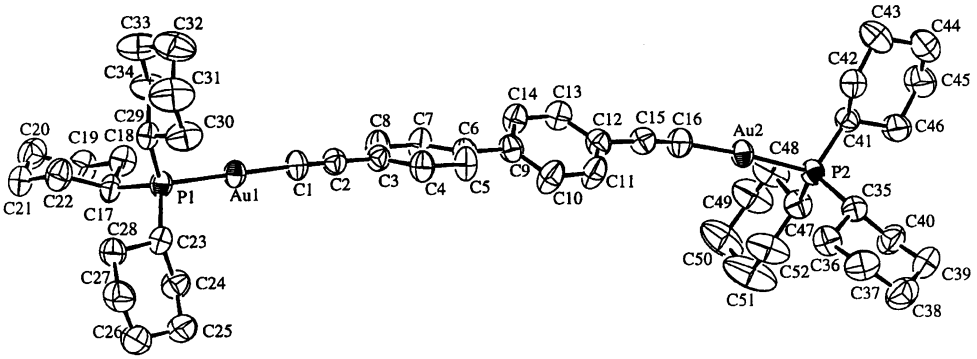

Figure 3. Perspective view of **9** (50% thermal ellipsoids). Selected bond lengths (Å) and angles (deg): Au(1)—P(1) 2.291(2), Au(2)—P(2) 2.289(2), Au(1)—C(1) 1.992(7), Au(2)—C(16) 2.017(7), C(1)≡C(2) 1.223(10), C(15)≡C(16) 1.177(10), P(1)—Au(1)—C(1) 176.9(2), P(2)—Au(2)—C(16) 175.7(2), Au(1)—C(1)≡C(2) 177.9(7), Au(2)—C(16)≡C(15) 173.8(7), C(1)≡C(2)—C(3) 179.0(8), C(16)≡C(15)—C(12) 175.5(8).

Table 1. Crystallographic Data for **3**, **4**, and **9**·MeOH·H_2O

	3	**4**	**9**·MeOH·H_2O
formula	$AuC_{32}H_{42}P$	$AuC_{34}H_{42}P$	$Au_2C_{53}H_{80}O_2P_2$
M_w	654.62	678.65	1205.09
crystal color	colorless	yellow	pale yellow
crystal size [mm]	0.25 × 0.15 × 0.07	0.25 × 0.15 × 0.07	0.30 × 0.15 × 0.10
crystal system	monoclinic	orthorhombic	triclinic
space group	$P2_1/n$ (no. 14)	*Pbca* (no. 61)	$P\bar{1}$ (no. 2)
a [Å]	13.273(1)	18.663(3)	13.284(2)
b [Å]	17.234(2)	19.047(3)	14.460(2)
c [Å]	25.080(2)	16.774(3)	15.618(3)
α [deg]	90	90	97.15(2)
β [deg]	94.68(1)	90	100.99(2)
γ [deg]	90	90	115.93(2)
V [Å^3]	5718(1)	5962(1)	2574(1)
Z	8	8	2
μ [cm^{-1}]	52.37	50.25	58.12
D_c [g cm^{-3}]	1.521	1.512	1.555
$2\theta_{max}$ [deg]	50	51	51
no. of reflns with $I > 3\sigma(I)$	5271	4300	7325
no. of parameters	613	325	531
R,[a] R_w[b]	0.028, 0.034	0.030, 0.040	0.047, 0.065
GOF	1.09	1.63	1.62

[a] $R = \Sigma(|F_o| - |F_c|)/\Sigma|F_o|$. [b] $R_w = [\Sigma w(|F_o| - |F_c|)^2/\Sigma w|F_o|^2]^{1/2}$.

in analogous gold(I) arylacetylide complexes.[5a−g,15a,c,17,19] The C(2)−C(3) distance between the two acetylide groups in **2** is 1.383(7) Å, which is comparable to those observed in Ru(C≡CC≡CPh)(PPh_3)$_2$Cp (1.389(6) Å)[20] and related M−(C≡C)$_2$−H (M = Au,[21a] Fe,[21b] Ru[21c]) (1.374(8)−1.386(3) Å) complexes. In complex **4**, the two phenyl rings separated by an acetylide unit are virtually coplanar with a dihedral angle of ∼4°. This implies that the π orbitals within the [C≡C-1,4-C_6H_4C≡CPh] fragment can undergo favorable overlap in the crystal lattice, and hence, extended π delocalization is likely. In contrast, the adjacent phenyl rings in complex **3** (dihedral angles ∼29 and 20°) and **9**·MeOH·H_2O (dihedral angle ∼30°) are skewed with respect to each other because of steric repulsion between proximal hydrogen atoms of the phenyl rings. No close intermolecular gold···gold contacts (<3.6 Å) are found in the crystal lattices of the structurally characterized gold(I) complexes in this work; as expected, the large cone angle (170°)[22] of the tricyclohexylphosphine ligand disfavors metal−metal and/or ligand−ligand aggregation.

Electronic Absorption Spectroscopy. The electronic absorption data of complexes **1**−**12** are summarized in Table 2 (for data of corresponding free arylacetylenes, see Supporting Information). Figure 4 shows the absorption spectra of **1a**, **2**, and **4**−**6** in dichloromethane solution. The absorption spectra of **1a** and phenylacetylene are similar in the 245−300 nm spectral region, but the absorption peaks of the former occur at slightly lower energies with higher extinction coefficients. For **1a**, four absorption peak maxima are observed at 255, 267, 281, and 290 nm. Similar absorption bands have been reported for Au(L)(C≡CPh) (L = PPh_3,[5a] PMe_3[5d]), {Au(C≡CPh)}$_2$(μ-L−L) (L−L = 1,2-bis(diphenylphosphino)ethane (dppe)[5a] and bis-(dimethylphosphino)methane (dmpm)[5d]), and Au(C≡CPh)-($CNC_6H_3Me_2$-2,6).[5c] We note that for (Cy_3P)AuC≡CAu(PCy_3),[6a] the [5d(Au)] → [6p(Au), π*(phosphine)] transitions occur at

(17) (a) Whittall, I. R.; Humphrey, M. G.; Houbrechts, S.; Persoons, A.; Hockless, D. C. R. *Organometallics* **1996**, *15*, 5738−5745. (b) Naulty, R. H.; Cifuentes, M. P.; Humphrey, M. G.; Houbrechts, S.; Boutton, C.; Persoons, A.; Heath, G. A.; Hockless, D. C. R.; Luther-Davies, B.; Samoc, M. *J. Chem. Soc., Dalton Trans.* **1997**, 4167−4174.

(18) Muir, J. A.; Muir, M. M.; Pulgar, L. B.; Jones, P. G.; Sheldrick, G. M. *Acta Crystallogr.* **1985**, *C41*, 1174−1176.

(19) (a) Jia, G.; Puddephatt, R. J.; Scott, J. D.; Vittal, J. J. *Organometallics* **1993**, *12*, 3565−3574. (b) Irwin, M. J.; Jia, G.; Payne, N. C.; Puddephatt, R. J. *Organometallics* **1996**, *15*, 51−57. (c) MacDonald, M. A.; Puddephatt, R. J.; Yap, G. P. A. *Organometallics* **2000**, *19*, 2194−2199.

(20) (a) Bruce, M. I.; Hall, B. C.; Kelly, B. D.; Low, P. J.; Skelton, B. W.; White, A. H. *J. Chem. Soc., Dalton Trans.* **1999**, 3719−3728. (b) Low, P. J.; Bruce, M. I. *Adv. Organomet. Chem.* **2001**, *48*, 71−288.

(21) (a) Bruce, M. I.; Hall, B. C.; Skelton, B. W.; Smith, M. E.; White, A. H. *J. Chem. Soc., Dalton Trans.* **2002**, 995−1001. (b) Akita, M.; Chung, M. C.; Sakurai, A.; Sugimoto, S.; Terada, M.; Tanaka, M.; Moro-oka, Y. *Organometallics* **1997**, *16*, 4882−4888. (c) Sun, Y.; Taylor, N. J.; Carty, A. J. *Organometallics* **1992**, *11*, 4293−4300.

(22) Tolman, C. A. *Chem. Rev.* **1977**, *77*, 313−348.

Table 2. Photophysical Data for **1**−**12**

complex	medium (T, K)	λ^{abs}, nm (ϵ_{max}, dm^3 mol^{-1} cm^{-1})	λ^{em}, nm	ϕ_{em} (τ, μs)[a]
1a	CH_2Cl_2 (298)	255 (14 140), 267 (27 440), 281 (28 490), 290 (10 190) (sh)	419 (max), 439, 446, 458, 483 (sh)	0.08 (18)
	MeOH/EtOH (77)		415 (max), 436, 446, 455, 469, 479, 491, 507	
	solid (298)		421 (max), 442, 451, 462, 474 (sh), 485, 497, 511 (sh)	0.22 (96)
1b	CH_2Cl_2 (298)	254 (13 140) (sh), 265 (23 650), 278 (23 930), 287 (11 930) (sh)	418, 437, 444 (max), 456, 478 (sh)	0.03 (16)
	solid (298)		420 (max), 439, 447, 459, 483, 496 (sh)	0.30 (145)
1c	CH_2Cl_2 (298)	248 (7550) (sh), 260 (15 440), 272 (28 700), 284 (29 760), 291 (21 650) (sh)	432 (max), 454 (sh), 461, 474, 497 (sh)	0.04 (16)
	solid (298)		427 (max), 448, 457, 469, 483 (sh), 493, 506 (sh), 523 (sh), 538 (sh)	0.20 (25)
1d	CH_2Cl_2 (298)	245 (6270) (sh), 258 (14 930), 269 (27 570), 281 (28 860), 290 (19 090) (sh)	424 (max), 445 (sh), 454, 463, 489 (sh)	0.04 (11)
	solid (298)		422, 444, 452, 464, 476 (max), 503, 515, 529 (sh), 548 (sh), 562 (sh)	0.26 (92)
2	CH_2Cl_2 (298)	247 (68 360), 255 (56 910), 262 (10 600) (sh), 278 (19 510), 294 (33 340), 313 (30 470), 353 (230)	466 (max), 491, 499, 519, 545, 584	0.03 (24)
	MeOH/EtOH (77)		459 (max), 482, 495, 511, 539, 557, 577	
	solid (298)		466 (max), 491, 502, 519, 548, 564, 584	0.008 (25)
3	CH_2Cl_2 (298)	264 (11 020) (sh), 277 (24 850) (sh), 294 (43 570), 304 (45 150)	330, 344 (max),[b] 495 (max),[c] 531, 573 (sh)	0.005 (7),[b] 0.04 (33)[c]
	solid (298)		350, 367 (max),[b] 494 (max),[c] 528, 532 (sh), 568 (sh)	0.01 (1.9),[b] 0.16 (209)[c]
	MeOH/EtOH (77)		321, 336 (max),[b] 484 (max),[c] 517	
4	CH_2Cl_2 (298)	248 (6510), 281 (16 100) (sh), 295 (33 770) (sh), 313 (59 540), 322 (47 110) (sh), 335 (55 180)	343 (max),[b] 356, 368 (sh), 512 (max),[c] 544, 556, 575 (sh)	0.08 (47),[b] 0.02 (114)[c]
	MeOH/EtOH (77)		336 (max),[b] 350, 354 (sh), 363, 378, 385 (sh), 395 (sh), 507 (max),[c] 530 (sh), 538, 552, 569, 589, 608	
	solid (298)		349, 364, 368, 376 (max),[b] 392, 399, 409, 516 (max),[c] 548, 561, 579 (sh)	(1.5),[b] (3.0)[c]
5	CH_2Cl_2 (298)	329 (74 270), 339 (83 680), 350 (75 310), 363 (64 850)	375, 390 (max),[b] 547 (max),[c] 584	0.66[d] (19),[b] (92)[c]
	MeOH/EtOH (77)		369 (max),[b] 387, 400, 419 (sh), 540 (max),[c] 577, 594 (sh), 615 (sh)	(0.3),[b] (0.4)[c]
	solid (298)		383, 406, 415 (max),[b] 432	(4)[b]
6	CH_2Cl_2 (298)	275 (22 210), 354 (102 940), 374 (69 110) (sh)	390 (max),[b] 407	0.69[b], (0.29)[b]
	MeOH/EtOH (77)		384 (max),[b] 406, 418 (sh), 436 (sh), 552 (max),[c] 592	(0.36),[b] (14.3)[c]
	solid (298)		400, 424, 436 (max), 456	(0.30)[b]
7	CH_2Cl_2 (298)	254 (13 690), 267 (27 200), 281 (32 520), 311 (1030) (sh)	408 (max), 430, 445, 467 (sh), 491 (sh)	0.02 (6)
	CH_3CN (298)	252 (11 620), 266 (24 060), 280 (28 950), 302 (510) (sh)	408 (max), 433, 444, 465 (sh), 491 (sh)	0.02 (5)
	solid (298)		410 (max), 429, 438, 448, 471, 481, 495, 521	0.03 (16)
8	CH_2Cl_2 (298)	288 (32 000) (sh), 304 (80 900), 323 (130 600)	488 (max), 517, 527, 547 (sh), 560 (sh), 580 (sh)	0.05 (81)
	MeOH/EtOH (77)		482 (max), 492, 502, 511, 523, 535	
	solid (298)		493 (max), 513 (sh), 523, 535, 549, 570, 584, 614 (sh)	0.03 (66)
9	CH_2Cl_2 (298)	323 (72 700)	361 (max),[b] 376, 391 (sh), 536 (max),[c] 574, 605 (sh)	0.08 (25),[b] 0.02 (76)[c]
	MeOH/EtOH (77)		363 (max),[b] 382, 403, 532 (max),[c] 558, 569, 581, 599, 614, 627, 642 (sh)	
	solid (298)		383 (max),[b] 403, 535 (max),[c] 573, 603 (sh)	0.02 (1.6),[b] 0.02 (71)[c]
10	CH_2Cl_2 (298)	315 (60 950), 325 (66 670), 335 (88 760), 345 (74 290), 360 (90 290)	366 (max),[b] 383, 394 (sh), 413 (sh), 540 (max),[c] 575	0.42[d] (49),[b] (192)[c]
	MeOH/EtOH (77)		361 (max),[b] 377, 381 (sh), 393, 411, 430 (sh), 450 (sh), 535 (max),[c] 572, 584 (sh), 605 (sh)	(0.3),[b] (0.2)[c]
	solid (298)		372 (sh), 394 (sh), 404 (max),[b] 421, 440 (sh), 542 (max),[c] 576, 589 (sh), 609 (sh)	(16),[b] (124)[c]
11	CH_2Cl_2 (298)	295 (23 110) (sh), 312 (38 980) (sh), 339 (78 950) (sh), 353 (96 570), 376 (64 430) (sh)	387 (max),[b] 407, 558 (max),[c] 599 (sh), 675	0.57[d]
	butyronitrile (77)		383 (max),[b] 402, 408, 420, 429 (sh), 440, 449, 462, 554 (max),[c] 579, 591 (sh), 611 (sh), 634 (sh), 673	(0.51),[b] (1.38)[c]
	solid (298)		421 (sh), 466 (max)	
12	CH_2Cl_2 (298)	290 (32 950), 358 (126 160), 375 (102 460) (sh)	397 (max), 417	0.70[b] (0.29)[b]
	MeOH/EtOH (77)		388, 419 (max),[b] 575 (max),[c] 620 (sh)	(0.36),[b] (57.6)[c]
	solid (298)		427 (sh), 443 (max),[b] 462 (sh), 586 (max)[c]	(2.05),[b] (5.27)[c]

[a] Lifetime was measured at peak maximum. [b] Fluorescence. [c] Phosphorescence. [d] Total emission quantum yield.

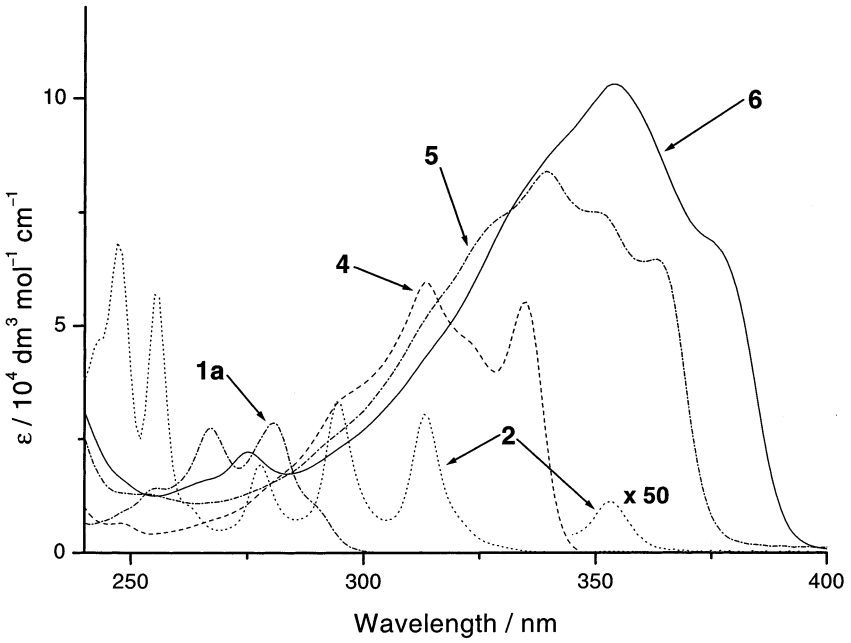

Figure 4. Electronic absorption spectra of **1a**, **2**, and **4**−**6** in CH_2Cl_2 at 298 K.

270 and 283 nm (ϵ = 6840 and 3500 dm^3 mol^{-1} cm^{-1}, respectively). However, these extinction coefficients are significantly lower than those observed for the band maxima at 267, 281, and 290 nm for **1a** ($\epsilon > 10^4$ dm^3 mol^{-1} cm^{-1}). We therefore assign the absorptions of **1a** as predominantly [PhC≡C$^-$] transitions that are red-shifted in energy through Au−C bonding interactions.[5g] The spacings between the four maxima at 255−290 nm are 1762, 1866, and 1105 cm^{-1}, which correspond to two kinds of vibrational stretching frequencies (i.e. acetylenic and phenyl). Interestingly, the absorption spectra of **1b**−**d** (see Supporting Information) with electron-withdrawing and -donating aryl substituents are similar to that of **1a**; hence, the substituent on the phenyl ring imparts minimal effect on the electronic transition energies. Complex **7** exhibits vibronically structured absorptions with peak maxima at 254, 267, and 281 nm. The vibrational spacings (1917 and 1866 cm^{-1}) appear in the range expected for C≡C stretching in the excited state, and these bands are assigned as predominantly $^1(\pi\pi^*)$ acetylenic transitions. An additional peak at 311 nm with a relatively small extinction coefficient ($\epsilon \approx 1030$ dm^3 mol^{-1} cm^{-1}) is tentatively assigned to a $^3(\pi\pi^*)$ acetylenic transition.

In the homologous series $(Cy_3P)Au(C{\equiv}C\text{-}1,4\text{-}C_6H_4)_{n-1}(C{\equiv}CPh)$ (n = 1 (**1a**), 2 (**4**), 3 (**5**), 4 (**6**)), the 0−0 absorption energy is red-shifted from **1a** to **6**, as depicted in Figure 4. Their lowest energy dipole-allowed transitions are similar, and, as discussed for **1a** above, are assigned to transitions that involve distortion of the acetylenic and phenyl groups in the excited state. The shifts to lower energies are due to greater conjugation across the $[(C{\equiv}C\text{-}1,4\text{-}C_6H_4)_{n-1}(C{\equiv}CPh)]$ fragment with increasing n values. In addition, the red shift of the absorption band relative to the free arylacetylene decreases for greater n values.

The absorption spectrum of complex **2** in dichloromethane (Figure 4) shows one shoulder (262 nm) and three intense bands (278, 294, and 313 nm), for which the progressional spacings are 2196, 1958, and 2065 cm^{-1}, respectively. These spacings can be ascribed to a single mode, namely ν(C≡C). In the absorption spectrum of HC≡CC≡CPh in hexane, absorptions at 242−284 nm with vibrational spacings of ∼2000 cm^{-1} are observed. These transitions are assigned to the spin-allowed $\pi \rightarrow \pi^*$ transition of the diacetylene unit. In the low-energy region, **2** exhibits a weak absorption band at 353 nm ($\epsilon \approx 230$ dm^3 mol^{-1} cm^{-1}); we tentatively assigned this to a spin-forbidden $\pi \rightarrow \pi^*$ transition. The intensity of this normally undiscernible band has apparently been enhanced by the heavy-atom effect of Au(I). Overall, a red shift of the $\pi\pi^*$ excited-state energy is observed from [PhC$_2^-$] to [PhC$_4^-$].

Complex **3** exhibits two absorption shoulders at 264 and 277 nm and two peak maxima at around 294 and 304 nm in dichloromethane. In contrast, free HC≡C-1,4-C_6H_4Ph shows only a broad band centered at 273 nm. Coordination of 4-ethynylbiphenyl to $[Au(PCy_3)]^+$ hence results in enhanced $\pi \rightarrow \pi^*$ transitions for the [C≡C-1,4-C_6H_4Ph] moiety. Compared with those of **1a**, the absorption peak maxima of **3** are red-shifted and more diffused. Complex **9** displays a broad band at 323 nm, and the corresponding free diacetylene also shows an unresolved band at 290 nm. The electronic transition presumably involves low-frequency torsional modes arising from the twisting of the two phenyl rings in the $\pi\pi^*$ excited state.[23] The binuclear complex **8** exhibits three absorption peak maxima at 288, 304, and 323 nm (spacings 1828 and 1935 cm^{-1}); they are slightly red-shifted from the absorption of 1,4-diethynylbenzene at 249 (sh), 260, and 273 nm in dichloromethane and are assigned to the $^1(\pi\pi^*)$ transition localized on the acetylenic unit. The absorption spectra for **10** and **11** show vibronic structures with spacings of 865−1847 cm^{-1} that are very similar to the corresponding arylacetylenes. These absorption bands are likewise assigned as $^1(\pi\pi^*)$ transitions involving acetylenic and phenyl units. In the series $(Cy_3P)Au(C{\equiv}C\text{-}1,4\text{-}C_6H_4)_nC{\equiv}CAu(PCy_3)$ (n = 1 (**8**), 2 (**10**), 3 (**11**), 4 (**12**)), the absorption bands are red-shifted when n increases, and the red shift in absorption energies compared to that of the free ligands decreases with increasing n values (see Supporting Information).

(23) Suppan, P. *Chemistry and light*; Royal Society of Chemistry: Cambridge, U.K., 1994; p 76.

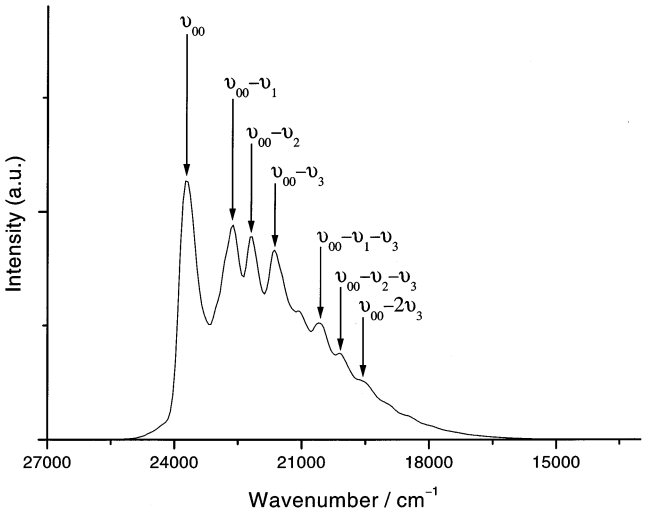

Figure 5. Solid-state emission spectrum of **1a** at 298 K (λ_{ex} = 280 nm).

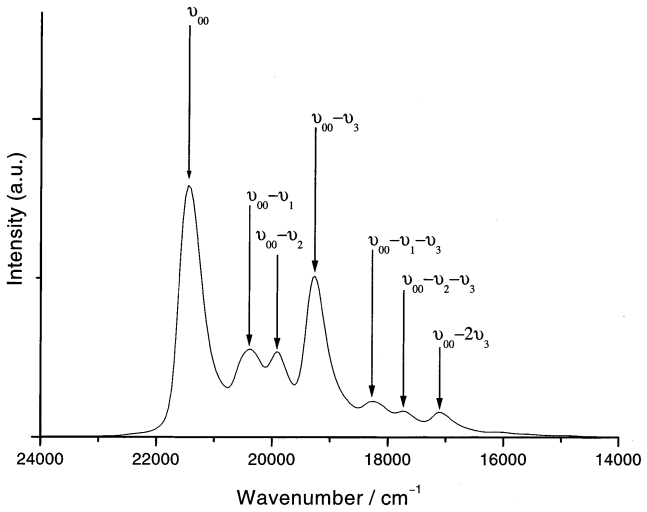

Figure 6. Solid-state emission spectrum of **2** at 298 K (λ_{ex} = 313 nm).

Steady-State Emission Spectroscopy. The excitation of complexes **1**−**12** at λ > 280 nm in the solid state and in fluid solutions at 298 K produces intense blue to yellow emissions; the spectral data are listed in Table 2. For complexes with short arylacetylide chains (**1a**−**d**, **2**, **7**, and **8**), their spectra are dominated by phosphorescence in the visible region. The solid-state emission spectra of **1a** and **2** at 298 K are given in Figures 5 and 6, respectively (see Supporting Information for **8**). The spectra display well-resolved vibronic structures, and three types of vibrational spacings, ν_1 (∼1100 cm^{-1}), ν_2 (∼1600 cm^{-1}), and ν_3 (∼2100 cm^{-1}), are identified. These spacings are attributed to the ground-state phenyl ring deformation, symmetric phenyl ring stretch, and C≡C stretching frequencies, respectively, and clearly correlate with the peak frequencies observed in the Raman spectra (for **1a**, 1173, 1598, and 2117 cm^{-1}; for **2**, 1178, 1596, 2070, and 2192 cm^{-1}). The ν_{00} ($0' \rightarrow 0$ emission energy), ν_1, ν_2, and ν_3 deduced from the solid state or 77 K glassy emission spectra are listed in Table 3. Similar findings had previously been observed for the Au(PPh$_3$)(C≡CPh)[5a] and [Pt(PEt$_3$)$_2$(C≡CPh)$_2$][24] derivatives. The observed large Stokes shifts of the emissions from the dipole-allowed absorptions, plus the long emission lifetimes (in the microsecond regime), are indicative of their triplet parentage, and they are thus assigned to the $^3(\pi\pi^*)$ excited states of the arylacetylide ligands. It is appropriate to highlight the role of the [Au(PCy$_3$)]$^+$ fragment, which introduces spin−orbit coupling and facilitates the observation of arylacetylide triplet emissions at room temperature. In our recent work on the binuclear gold(I) complexes (Cy$_3$P)Au(C≡C)$_n$Au(PCy$_3$) (n = 1−4), the acetylenic $^3(\pi\pi^*)$ emissions localized on the (C≡C)$_n^{2-}$ chain can be "switched on" by ligation to [Au(PCy$_3$)]$^+$.[6] In this study, the incorporation of aryl ring(s) into the (C≡C)$_n^{2-}$ moiety increases the vibrational modes that are observed in the emission spectra.

Table 3. ν_{00} and ν_1−ν_3 Stretching Frequencies for Solid-State Emissions at 298 K

complex	ν_{00} (cm^{-1})	ν_1 (cm^{-1})	ν_2 (cm^{-1})	ν_3 (cm^{-1})
1a	23 752	1128	1580	2107
1b	23 809	1030	1438	2023
1c	23 419	1098	1538	2098
1d	23 696	1174	1573	2145
2	21 459	1093	1539	2192
3	28 571[a]	- -	1324[a]	- -
	20 242[b]	- -	1446[b]	- -
4[c]	29 761[a]	1190[a]	1513[a]	2213[a]
	19 723[b]	1136[b]	1608[b]	2149[b]
5[c]	27 100[a]	1261[a]	- -	2100[a]
	18 518[b]	1187[b]	1683[b]	2258[b]
6[c]	26 042[a]	- -	1411[a]	2118[a]
	18 116[b]	1224[b]	- -	- -
7	24 390	1080	1559	2069
8	20 283	1163	1592	2069
9	26 109[a]	1296[a]	- -	- -
	18 691[b]	1239[b]	- -	2108[b]
10[c]	27 700[a]	1175[a]	1454[a]	2255[a]
	18 691[b]	1209[b]	1568[b]	2163[b]
11[d]	26 109[a]	1234[a]	1600[a]	2300[a]
	18 050[b]	1130[b]	1684[b]	2278[b]
12[c]	25 773[a]	- -	- -	1907[a]
	17 391[b]	1262[b]	- -	- -

[a] Fluorescence. [b] Phosphorescence. [c] In MeOH/EtOH 77 K glass. [d] In butyronitrile 77 K glass.

For complexes with longer arylacetylide chains (**3**−**6** and **9**−**12**), dual emissions (high-energy, 330−407 nm; low-energy, 495−558 nm) are recorded. Figure 7 shows the emission spectra of **4**, **5**, **10**, and **11** in dichloromethane at 298 K. To further examine these emissions, the excitation spectra of **4** (Figure 8)[25] and **11** (see Supporting Information) in 77 K glassy solutions have been obtained. Well-resolved vibronic fine structures are detected which match the corresponding room temperature absorption spectra. For **4**, the 298 nm shoulder and 318 nm peak maximum, which are absent in the absorption spectrum, appear in the 77 K excitation spectrum. Three kinds of progressional spacings (∼1110, 1600, and 2100 cm^{-1}) can clearly be identified and attributed to the stretching frequencies of the phenyl and acetylenic groups in the $^1(\pi\pi^*)$ excited state. The excitation spectra monitored at the high- and low-energy emission bands have been found to be identical, suggesting that both emissions originate from the same absorbing state. The

(24) Sacksteder, L.; Baralt, E.; DeGraff, B. A.; Lukehart, C. M.; Demas, J. N. *Inorg. Chem.* **1991**, *30*, 2468−2476.

(25) Complex **4** is sparingly soluble in MeOH/EtOH, and all solutions were carefully filtered before excitation and emission measurements (the absorbance at 313 nm is maintained at ∼0.1 to reduce the possibility of aggregate formation). A solution of **4** in MeOH/EtOH/DMF (5:5:1), in which the compound readily dissolves, was also prepared, and the 77 K excitation and emission spectra of this glassy solution were basically identical to those of the MeOH/EtOH glass. Furthermore, the emission spectra of **4** in solid, fluid (CH_2Cl_2), and glassy states are very similar. It is, therefore, highly unlikely that the dual emission originates from aggregate species or a small amount of unmetalated impurity within an aggregate.

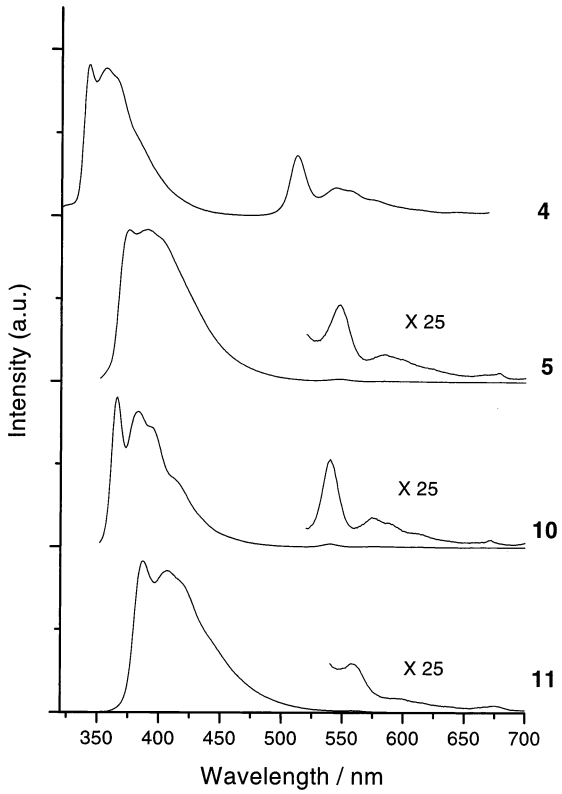

Figure 7. Emission spectra of **4**, **5**, **10**, and **11** in CH_2Cl_2 at 298 K (λ_{ex} = 313, 339, 335, and 353 nm, respectively).

high-energy emission, however, exhibits lifetime in the microsecond regime, and we tentatively assign it to "delayed fluorescence". In principle, delayed fluorescence can be produced by two types of pathways, namely thermally induced delayed fluorescence ($T_1 \rightarrow S_1$) and triplet−triplet annihilation ($T_1 + T_1 \rightarrow S_1 + S_0$, where S_0, S_1, and T_1 are the ground state and the lowest singlet and triplet excited states, respectively).[26] On the basis of the shorter lifetimes of the high-energy emissions (Table 2), we suggest that the delayed fluorescence detected in this work is generated by triplet−triplet annihilation.[27]

Minimal solvatochromic effects on the absorption and emission spectra of these complexes have been detected. As a prototypical example, the emission spectra of **2** in various solvents at 298 K are shown in the Supporting Information. The quantum yields (ϕ_{em}) and lifetimes (τ) decrease in the order: CH_2Cl_2 (0.03; 24 μs) ≈ THF (0.03; 22 μs) > CH_3CN (0.01; 12 μs) ≈ MeOH (0.01; 12 μs). In addition, the complex concentration imparts only a minor effect upon the emission quantum yields and lifetimes. This is consistent with the self-quenching rate constant k_{sq} of 1.9×10^7 dm^3 mol^{-1} s^{-1} for the emission of **2** in dichloromethane (determined by the Stern−Volmer equation: $1/\tau = 1/\tau_0 + k_{sq}[M]$, where τ_0 is the lifetime at infinite dilution and [*M*] is the complex concentration).

Electrochemical and Photoredox Properties. The electrochemical properties of complexes **1**−**4** and **7**−**9** have been examined by cyclic voltammetry in CH_2Cl_2. In general, one to two irreversible oxidation waves are displayed at 0.8−1.0 V versus $Fc^{0/+}$. For example, **3** exhibits irreversible oxidation waves at 0.81 and 0.96 V, and **8** shows an irreversible peak at 0.92 V versus $Fc^{0/+}$.

Table 4. Bimolecular Rate Constants for Oxidative Quenching of **1a** by Pyridinium Acceptors in Acetonitrile (0.1 mol dm^{-3} ^{n}Bu$_4$NPF$_6$) at 298 K

quencher[a]	$E°(A^+/A)$[b] (vs SSCE)	k_q (dm^3 mol^{-1} s^{-1})	k_q'[c] (dm^3 mol^{-1} s^{-1})	ln k_q'
N,*N*′-dimethyl-4,4′-pyridinium	−0.45	9.97×10^9	1.99×10^{10}	23.71
4-cyano-*N*-methylpyridinium	−0.67	7.45×10^9	1.19×10^{10}	23.20
4-amido-*N*-ethylpyridinium	−0.93	5.17×10^9	6.97×10^9	22.66
3-amido-*N*-benzylpyridinium	−1.07	3.51×10^9	4.26×10^9	22.17
3-amido-*N*-methylpyridinium	−1.14	3.12×10^9	3.70×10^9	22.03
N-ethylpyridinium	−1.37	8.55×10^8	8.93×10^8	20.61
2,6-dimethyl-*N*-methylpyridinium	−1.52	2.64×10^8	2.68×10^8	19.41
2,4,6-trimethyl-*N*-methylpyridinium	−1.67	3.86×10^7	3.86×10^7	17.47

[a] All quenchers are hexafluorophosphate salts. [b] Reference 28. [c] $(1/k_q') = (1/k_q) - (1/k_d)$, where k_d is the diffusion-limited rate constant, taken to be 2×10^{10} dm^3 mol^{-1} s^{-1}. Errors for k_q and k_q' are estimated to be ±5%.

The $^3(\pi\pi^*)$ states of these gold(I) arylacetylide complexes are strong photoreductants.[5a,c] Because they do not display reversible electrochemistry, their excited-state reduction potentials cannot be precisely evaluated using spectroscopic and electrochemical data. Oxidative quenching experiments of the triplet emissions of **1a**, **2**, and **4** in acetonitrile by a series of pyridinium acceptors (A^+)[28] have therefore been undertaken. Table 4 lists the quenching data for **1a**, and a nonlinear least-squares fitting of ln k_q' versus $E°$ (A^+/A) using the Rehm−Weller model (equation 1) has been performed (Figure 9) (for **2** and **4**, see Supporting Information).

$$(RT/F)\ln k_q' = (RT/F)\ln(K\kappa\nu) - \Delta G/2 - [(\Delta G/2)^2 + (\lambda/4)^2]^{1/2} \quad (1)$$

Here, $K = k_d/k_{-d}$, which is approximately 1−2 dm^3 mol^{-1} and κ, ν, and λ are the transmission coefficient, nuclear frequency, and reorganization energy for electron transfer, respectively; ΔG is the standard free-energy change of the reaction given by eq 2. The work terms ω_p and ω_r associated with bringing the reactants or products to mean separation are small and are neglected in this case.

$$\Delta G = E°[\mathbf{Au}^+/\mathbf{Au}^*] - E°(A^+/A) + \omega_p - \omega_r \quad (2)$$

Thus, the excited-state reduction potentials $E°[\mathbf{Au}^+/\mathbf{Au}^*]$ (**Au** = **1a**, **2**, and **4**) are estimated to be −1.80, −1.28, and −1.17 V versus SSCE (or −2.11, −1.59, and −1.48 V versus $Fc^{0/+}$), respectively. For **1a** and **4**, these values correspond to those (less than −2.01 and −1.43 V versus $Fc^{0/+}$, respectively) estimated from the equation $E°[\mathbf{Au}^+/\mathbf{Au}^*] = E°[\mathbf{Au}^+/\mathbf{Au}] - E_{0-0}$, where E_{0-0} is calculated from the spectroscopic data (2.94 and 2.43 eV, respectively) and $E°[\mathbf{Au}^+/\mathbf{Au}]$ is approximated from E_{pa} obtained in cyclic voltammetry measurements (less than 0.93 and 1.00 V versus $Fc^{0/+}$, respectively).[29] The large

(26) Turro, N. J. *Modern Molecular Photochemistry*; The Benjamin/Cummings Publishing Company: Menlo Park, California, 1978; pp 146−148 and 343−344.

(27) We have also examined the relationship between the fluorescence to phosphorescence signal ratio and the energy of laser pulse at 266 nm excitation. When the energy of laser pulse was increased from 0.57×10^{-3} to 7.18×10^{-3} joule/pulse, the ratio of fluorescence to phosphorescence signal was observed to increase from 1.5 to 2.8. This is consistent with a triplet−triplet annihilation mechanism for the delayed fluorescence. We are grateful to the reviewers for suggesting this experiment.

(28) Marshall, J. L.; Stobart, S. R.; Gray, H. B. *J. Am. Chem. Soc.* **1984**, *106*, 3027−3029.

(29) Because the electrochemical oxidation is irreversible, only the E_{pa} of the oxidation wave is determined.

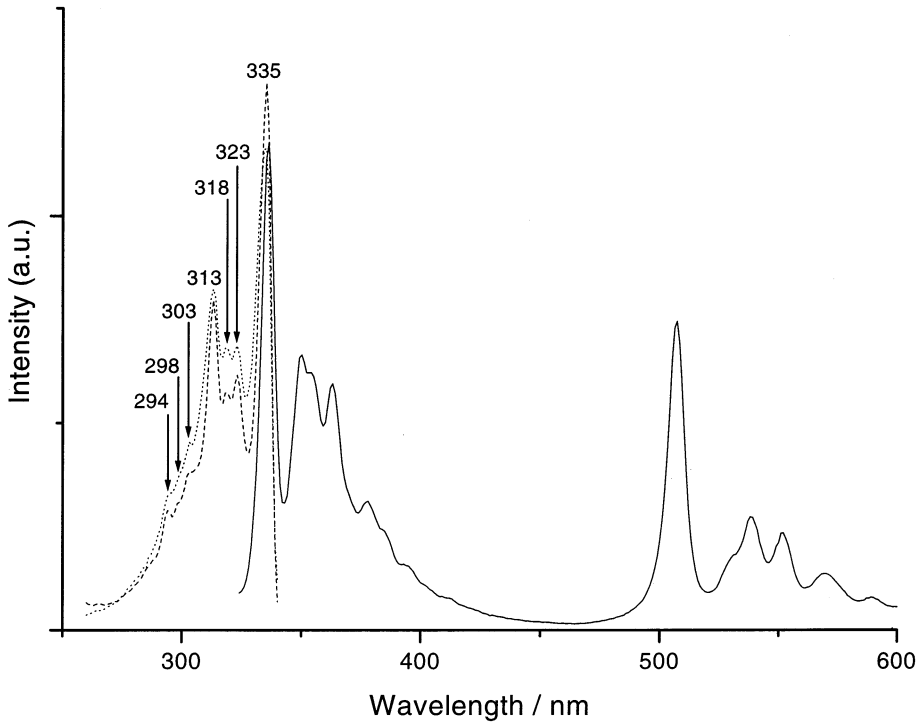

Figure 8. Excitation (λ_{em} = 350 (•••) and 506 (- - -) nm) and emission (—) (λ_{ex} = 313 nm) spectra of **4** in MeOH/EtOH (4:1) at 77 K.

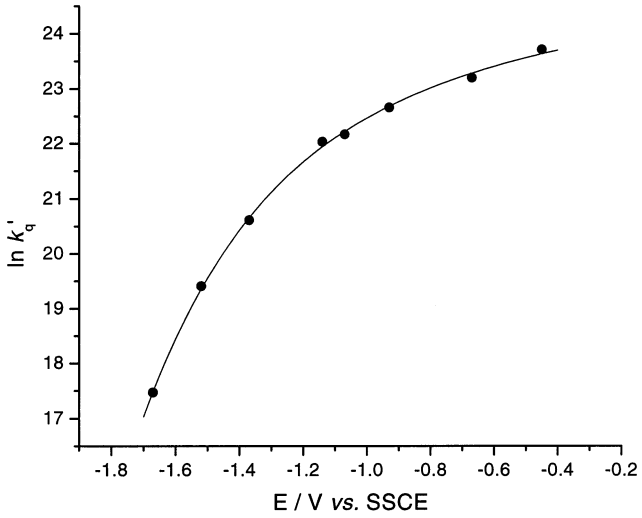

Figure 9. Plot of ln k_q' vs $E°(A^+/A)$ for the oxidative quenching of **1a** by pyridinium acceptors in acetonitrile: (+) experimental data and (—) theoretical curve.

negative values of $E°$[**Au**$^+$/**Au***] indicate the strongly reductive nature of the $^3(\pi\pi^*)$ excited states of arylacetylides.

Discussion

General Remarks. Gold(I) arylacetylide compounds are usually prepared according to two literature methods. The reactions of [Au—C≡CR]$_n$ and [Au—C≡C—Ar—C≡C—Au]$_n$ with isocyanide or phosphine ligands were employed by Puddephatt and co-workers to give mononuclear, binuclear, and polymeric derivatives.[19] Alternatively, the treatment of Au(PR$_3$)-Cl and Au$_2$(P—P)Cl$_2$ (P—P = diphosphine ligands) with terminal alkynes in the presence of a base can also afford acetylide complexes.[15] The method adopted in this work, using the stable and easily prepared Au(PCy$_3$)Cl as precursor, is direct and convenient; plus, no polynuclear gold(I) arylacetylide side products were isolated. The arylacetylide bonding mode is confirmed by IR/Raman spectroscopy and crystallographic studies. The high ν(C≡C) stretching frequency (2067−2188 cm^{-1}) as well as the bond lengths of Au−C$_\alpha$ (1.993(11)−2.03(1) Å) and C$_\alpha$≡C$_\beta$ (1.180(6)−1.223(10) Å) demonstrate the σ-bonding nature of the coordinated arylacetylide groups. While metal complexes of arylacetylide ligands and their polymers are well-documented, reports of well-defined molecular derivatives bearing repeating arylacetylide or "oligo(phenylene-ethynylene)" moieties such as complexes **6** and **12** are sparse in the literature.[30]

The $^3(\pi\pi^*)$ excited states of arylacetylides have been shown to exhibit rich photochemical reactivities. The excited-state reduction potentials of **1a**, **2**, and **4** (−1.80, −1.28, and −1.17 V versus SSCE respectively) span over a wide range, and the trend for $E°$ values follows the variation in triplet emission energies. The excited-state potential of **1a** is similar to $E°$[Au(C≡CPh)(CNC$_6$H$_3$Me$_2$-2,6)$^{+/*}$] (−1.62 V versus SSCE).[5c] The large negative values imply that these $^3(\pi\pi^*)$ excited states are strong photoreductants. It has been possible to tune the excited-state reduction potential by modifying the arylacetylide chain length, although a clear relationship linking these two parameters has not been determined. Since arylacetylenes are a well-established class of organic compounds with diverse structural and electronic properties, the Cy$_3$PAuC≡CR complexes described here represent a new family of metal-organic photoreductants with tunable triplet-state photophysical properties under ambient conditions.

Trends in Absorption Energies. The absorption spectra of virtually all of the gold(I) arylacetylide complexes studied in

(30) For an example of extended arylacetylide complexes, see [Ru(C≡C-1,4-C$_6$H$_4$)$_2$C≡CC$_6$H$_4$NO$_2$-4] species in: Hurst, S. K.; Cifuentes, M. P.; Morrall, J. P. L.; Lucas, N. T.; Whittall, I. R.; Humphrey, M. G.; Asselberghs, I.; Persoons, A.; Samoc, M.; Luther-Davies, B.; Willis, A. C. *Organometallics* **2001**, *20*, 4664−4675.

this work show vibronically structured absorption bands. Distinct similarities between the absorption spectra of free arylacetylenes and gold(I) arylacetylide derivatives indicate that the electronic transitions in the latter are intraligand in nature and localized on the coordinated arylacetylides. The red shifts in the absorption spectra relative to the free acetylenes are attributed to the nature of the Au(I)−C(arylacetylide) bonding interaction, which decreases the energy difference between the arylacetylide π and π^* orbitals. The different magnitudes for the spacings between the absorption peak maxima signify that the lowest dipole-allowed electronic transitions of the gold(I) arylacetylide complexes involve distortion of the phenyl and acetylenic groups in the excited states.

When the length of the π-conjugated system in the homologous series $(Cy_3P)Au(C{\equiv}C\text{-}1,4\text{-}C_6H_4)_{n-1}(C{\equiv}CPh)$ and $(Cy_3P)Au(C{\equiv}C\text{-}1,4\text{-}C_6H_4)_nC{\equiv}CAu(PCy_3)$ ($n = 1-4$) is increased, the corresponding absorption bands are red-shifted in agreement with a reduction in the $\pi \rightarrow \pi^*$ energy gap. The 0−0 absorption energies for the two homologous series have been plotted against $1/n$ ($n = 1-4$; see Supporting Information), and a linear relationship was obtained. By extrapolation, a limiting value for the absorption energy (i.e. for $n = \infty$) is estimated to be in the 399−411 nm range; this value approaches the absorption energy of alkyl-substitued PPEs in solution (388 nm).[31]

Singlet and Triplet Excited States: S_0-T_1 Energy Gap and Extrapolation to PPEs. Phosphorescence is observed in the emission spectra of gold(I) arylacetylide complexes, while delayed fluorescence becomes prominent for derivatives bearing long arylacetylide chains (**3**−**6** and **9**−**12**). The detected vibronic fine structure is in accordance with the assignment to arylacetylide $^3(\pi\pi^*)$ states. We have been able to tune the energy of phosphorescence by altering the functionality of the arylacetylide ligand. The substituent on the phenyl ring in **1a**−**d** exerts minimal effect on the emission energy, suggesting large acetylenic parentage in the $^3(\pi\pi^*)$ excited state. The emission energy of the gold(I) complexes in dichloromethane decreases in the order: **1a** (23 866 cm^{-1}) > **2** (21 459 cm^{-1}) > **8** (20 492 cm^{-1}) > **3** (20 202 cm^{-1}) > **4** (19 531 cm^{-1}) > **9** (18 657 cm^{-1}) > **10** (18 518 cm^{-1}) > **5** (18 281 cm^{-1}) > **6** (18 116 cm^{-1}) > **11** (17 889 cm^{-1}) > **12** (17 391 cm^{-1}).[32]

To examine the relationship between the phosphorescent emission energy and arylacetylide chain length, we have plotted $\Delta E(S_0 - T_1)$ (energy gap between S_0 and T_1) against $1/n$ [n is the number of repeating arylacetylide units in mononuclear (square) $(Cy_3P)Au(C{\equiv}C\text{-}1,4\text{-}C_6H_4)_{n-1}(C{\equiv}CPh)$ ($n = 1$ (**1a**), 2 (**4**), 3 (**5**), 4 (**6**)) and binuclear (circle) $(Cy_3P)Au(C{\equiv}C\text{-}1,4\text{-}C_6H_4)_nC{\equiv}CAu(PCy_3)$ ($n = 1$ (**8**), 2 (**10**), 3 (**11**), 4 (**12**)) complexes] to produce good linear fits (Figure 10). This allows extrapolation of the line to reveal an estimated $\Delta E(S_0 - T_1)$ value for infinite repeating units (i.e. [Cy_3PAu]-capped PPE) of ∼626 nm (1.98 eV) and ∼607 nm (2.04 eV) for the mono- and dinuclear species, respectively. We consider these two limiting $\Delta E(S_0 - T_1)$ values to be the same within experimental uncertainties. This can be compared to the observed $S_0 - T_1$ separations (i.e. phosphorescence) of 1.90−2.08 eV for poly-

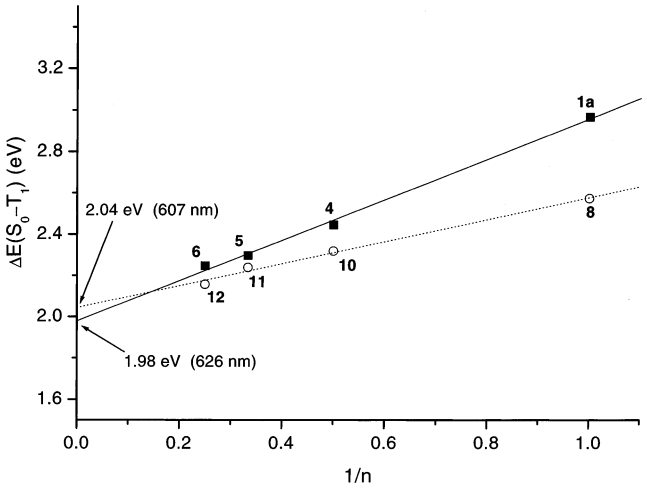

Figure 10. Plot of $\Delta E(S_0 - T_1)$ against $1/n$ (■ = mononuclear and ○ = dinuclear series).

(*p*-phenylene) derivatives[33] and around 1.9 eV for dialkoxy-substituted PPEs[4f] (both at ∼77 K in 2-methyltetrahydrofuran (Me-THF)).

A salient objective of this study is to gather in-depth information regarding the energy levels of arylacetylide $^1(\pi\pi^*)$ and $^3(\pi\pi^*)$ excited states. We have observed a good linear relationship between the lowest arylacetylide $^1(\pi\pi^*)$ excited-state energy $[\Delta E(S_0 - S_1)]$ and arylacetylide chain length ($1/n$; see Supporting Information), and the limiting value for $\Delta E(S_0 - S_1)$ is estimated to be 2.74−2.82 eV. Hence, by correlation of this value with $\Delta E(S_0 - T_1)$ (1.98−2.04 eV), the $\Delta E(S_1 - T_1)$ value for $n = \infty$ is estimated to be ∼0.8 eV. This corresponds directly with the $S_1 - T_1$ energy gap of 0.7 ± 0.1 eV reported by Friend and co-workers for a series of polymeric platinum(II) arylacetylide complexes and dialkoxy-substituted PPEs.[4d,f] Comparable $S_1 - T_1$ separations of 0.62−0.84 eV were observed for related poly(*p*-phenylene) materials by Bässler and co-workers,[33] while Monkman reported separations of 0.6−1.0 eV for a variety of π-conjugated polymers.[34] The $S_1 - T_1$ energy gaps for the arylacetylide gold(I) complexes studied herein (0.96−1.25 eV) are larger than the limiting value. This phenomenon was observed for monomeric and oligomeric platinum(II) arylacetylide analogues and has been attributed to the confinement of the S_1 state by Köhler et al.[4f] There is a linear relationship between the singlet- and triplet-state energies (see Supporting Information). From the linear least-squares fitting, the lowest triplet-state energy (T_1) for **4**−**6** and **10**−**12** can be expressed by the equation: $T_1 = 0.47S_1 + 0.70$. We can estimate the triplet excited-state energy of PPE materials by using the $S_1 - T_1$ energy gap (∼0.8 eV) derived in this work.[35] For example, by taking the fluorescent emission energy of poly(2,5-dihexyl-1,4-phenylene-ethynylene) in fluid solution (428 nm, 2.90 eV),[31] the energy of the phosphorescence is expected to be around 590 nm (2.10 eV).

(31) Mangel, T.; Eberhardt, A.; Scherf, U.; Bunz, U. H. F.; Müllen, K. *Macromol. Rapid Commun*. **1995**, *16*, 571−580.
(32) Because complexes **6** and **12** do not display phosphorescence in dichloromethane at 298 K, their phosphorescent emission energies are taken from 77 K alcoholic glasses.
(33) Hertel, D.; Setayesh, S.; Nothofer, H. G.; Scherf, U.; Müllen, K.; Bässler, H. *Adv. Mater*. **2001**, *13*, 65−70.
(34) Monkman, A. P.; Burrows, H. D.; Hartwell, L. J.; Horsburgh, L. E.; Hamblett, I.; Navaratnam, S. *Phys. Rev. Lett*. **2001**, *86*, 1358−1361.
(35) This estimate may be regarded as the approximate "intrinsic" value for the polymer, since macromolecular effects such as interchain interactions have not been considered; the estimated value may, therefore, be more appropriate for an isolated polymer chain in dilute solutions or inert matrixes. See: Cornil, J.; dos Santos, D. A.; Crispin, X.; Silbey, R.; Brédas, J. L. *J. Am. Chem. Soc*. **1998**, *120*, 1289−1299.

When compared with the emission spectra of the free arylacetylenes used in this work, which show fluorescence at 298−406 nm, phosphorescence has been "switched on" at ambient temperature by substitution of the terminal proton for a heavy gold atom, which induces intersystem crossing from singlet to triplet states. We have found that as the arylacetylide chain length increases, the intensity of the phosphorescence relative to fluorescence decreases; the results are depicted in Figure 7. This can be rationalized by the energy gap law, which states that the nonradiative decay rate increases exponentially upon decreasing the energy gap between two electronic states.[4e,36] Hence, the lowering of the triplet-state energy results in a faster nonradiative decay rate for the triplet state.

Comparison between Aliphatic and Aryl Phosphine Auxiliaries. It is pertinent to compare the emissive properties of the complexes described in this work with those of analogous gold(I) arylacetylide derivatives bearing arylphosphine ligands.[5] For the latter, which often display aurophilic interactions in their crystal lattices, the solid-state emissions can originate from a variety of different electronic excited states, such as $^3[\sigma(\mathrm{Au-P}) \rightarrow \pi^*(\mathrm{phosphine})]$, $^3[\mathrm{d}\sigma^* \rightarrow \mathrm{p}\sigma]$, or ligand-centered $^3[\pi \rightarrow \pi^*]$. Our strategy of employing the tricyclohexylphosphine ligand suppresses the aggregation of gold(I) centers, so that other possibilities are eliminated. Hence, the emissions of the gold(I) complexes can be confidently assigned to the $\pi\pi^*$ excited states of arylacetylide moieties.

Conclusion

Vibronically structured $\pi\pi^*$ transitions are observed in the absorption and emission spectra of the gold(I) arylacetylide derivatives reported in this work. The organic triplet emissions of arylacetylide groups have thus been "illuminated" at ambient conditions by ligation to the $[\mathrm{Au(PCy_3)}]^+$ fragment. The tunability of the arylacetylide $^3(\pi\pi^*)$ emission energy has been illustrated, while delayed $^1(\pi\pi^*)$ fluorescence for extended arylacetylide units is proposed to occur via a triplet−triplet annihilation mechanism. The singlet and triplet excited-state energies have been probed in a systematic manner using, in particular, two homologous series containing oligomeric arylacetylide moieties. Subsequent extrapolations to infinite repeating arylacetylide units (i.e. $(\mathrm{Cy_3P})$Au-capped PPE) have yielded valuable information regarding the photoluminescent nature of arylacetylide polymers ($S_0 - T_1$ and $S_1 - T_1$ energy separations of around 2.0 and 0.8 eV, respectively, have been estimated) and enabled comparisons with related π-conjugated polymeric materials. The $^3(\pi\pi^*)$ excited states of arylacetylides are powerful photoreductants. Since this class of compounds exhibit high quantum yields and tunable emission energies in the visible region, they may display potential applications as photonic materials.

(36) (a) Siebrand, W. *J. Chem. Phys.* **1967**, *47*, 2411−2422. (b) Englman, R.; Jortner, J. *Mol. Phys.* **1970**, *18*, 145−164.

Acknowledgment. We are grateful for financial support from the Research Grants Council of the Hong Kong SAR, China [HKU 7077/01P], The University of Hong Kong, and The Croucher Foundation (Hong Kong). We thank the reviewers for helpful comments and suggestions.

Supporting Information Available: Details of instrumentation and photophysical measurements. Perspective views of **1a**−**d**, **2**, **5**, **7**, and **8** and CIF data for all crystal structures. UV−Vis spectra of **1a**−**d** in CH_2Cl_2 at 298 K. UV−vis spectra of **8** and **10**−**12** in CH_2Cl_2 at 298 K. Emission spectrum of **8** in solid state at 298 K. Excitation and emission spectra of **11** in butyronitrile at 77 K. Normalized emission spectra of **2** in CH_3CN, CH_2Cl_2, MeOH, and THF at 298 K. Plots of ln k_q' versus $E°(A^+/A)$ for the oxidative quenching of **2** and **4** by pyridinium acceptors in acetonitrile. Plot of 0−0 absorption energy against $1/n$ for **1a**, **4** −**6**, **8**, and **10**−**12**. Plot of $\Delta E(S_0 - S_1)$ against $1/n$. Plot of $\Delta E(S_0 - S_1)$ against $\Delta E(S_0 - T_1)$ for **4**−**6** and **10**−**12**. Tables of selected bond lengths and angles of **1a**−**d**, **2**−**5**, **7**, **8**, and **9**·MeOH·H_2O; photophysical data for **1**−**12** (expanded) and free arylacetylenes; bimolecular rate constants for the oxidative quenching of **2** and **4** by pyridinium acceptors. Characterization data for **1b**−**d**, **2**−**5**, **7**, and **9**−**12**. This material is available free of charge via the Internet at http://pubs.acs.org.

JA0209417